iomac
International Operational Modal Analysis Conference
11th International Operational Modal Analysis Conference
20 - 23 May 2025 | Rennes, France

Using Scanning Laser Doppler Vibrometry for Experimental Frequency-based Substructuring

Marie Brøns [1]

[1] Department of Civil and Mechanical Engineering, Technical University of Denmark, maribr@dtu.dk

ABSTRACT
Frequency-based substructuring is a practical technique to predict the response of larger dynamic systems. Experimental substructuring is carried out today by measuring the response after a hammer impact with accelerometers on selected positions on the structures. The impacts are repeated in several positions on the structure (the rowing hammer principle). This work investigates the potential of using a scanning laser Doppler vibrometer (SLDV) instead. The classical accelerometer technique has proven to be efficient in many cases. It is, however, cumbersome to attach the many accelerometers. The virtual point (VP) transformation is often used when coupling complex structures, requiring a minimum of three three-directional sensors close to the interface (where the two substructures are to be connected). If the structure is small, it may not be possible. An SLDV is contactless, and the laser pointer is very small, which is why it is possible to have a fine grid of measurement points near the interface. However, to take advantage of the ”scanning” feature, attaching a shaker or piezoelectric-electric actuator is necessary. In this work, we design a novel numerical framework for SLDV/shaker testing, make the first preliminary SLDV tests, and discuss the benefits and limitations of this new approach.

Keywords: SLDV, frequency-based substructuring, virtual point, measurement accuracy

1. INTRODUCTION

Experimental Frequency-Based Substructuring (FBS) is a popular technique for predicting the dynamic response in complex structures [1]. By measuring the response in smaller and simpler-to-test parts and coupling these in the frequency domain, the response of larger systems can be predicted. Or, applied in reverse; a smaller part’s dynamics can be predicted by decoupling it from a larger structure [2]. In a design phase, FBS is useful. If one part is redesigned, an entire new measurement campaign can be avoided, as it is only necessary to retest the redesigned component. The classical approach is to use accelerometers and hammer impacting. Accelerometers are however cumbersome to attach and for some

structures too large to place near the interface. Attaching multiple accelerometers will also both affect the response, through the significant mass, and the many cables introduce additional damping. In this work, we investigate using an SLDV for FBS coupling instead. An SLDV can scan a large surface in a matter of minutes. It is contactless, introduces no extra damping nor additional mass to the system. In that way, it appears to be a great alternative to accelerometers. However, it also comes with some drawbacks. To be able to use the scanning-feature, a steady excitation source is needed, e.g. a piezo-electric actuator or a shaker. Such an excitation also affects the structure, and it is not easy to move around like a hammer. In the following, we introduce the equations needed to perform FBS and we introduce the concept of virtual point transformation (VPT). The VPT reduces the interface to a single point, making it a weakening of the interface. It is a very useful approach, but it also introduces assumptions, that take away some of the potential benefits of using an SLDV. We will address the VPT drawbacks in the following sections. Using a benchmark structure, we design a numerical experiments coupling two substructures, based on FRFs obtained from the interface surfaces, which we expect measurable with an SLDV. Here we demonstrate the drawbacks of the SLDV. To check the plausibility of the implementation, we make a first experiments with the SLDV, measuring a single surface of one of the substructures. We check the quality of the experimental data, the consistency to the model and reflect over the time and effort in setting the test up.

1.1. Frequency-based substructuring and virtual point transformation

The mathematics behind FBS are well documented in [1]. Here we use the *dual* Lagrangian multiplier approach. In short, we assume to have two systems A and B:

$$\begin{cases} \mathbf{u} = \mathbf{Y}^{\mathrm{A|B}}(\mathbf{f} - \mathbf{B}^{\mathrm{T}}\boldsymbol{\lambda}) \\ \mathbf{B}\,\mathbf{u} = \mathbf{0} \end{cases}, \qquad \mathbf{Y}^{\mathrm{A|B}} = \begin{bmatrix} \mathbf{Y}^{\mathrm{A}} & \mathbf{0} \\ \mathbf{0} & \mathbf{Y}^{\mathrm{B}} \end{bmatrix}, \tag{1}$$

where $\mathbf{u}$ is the displacement vector, $\mathbf{f}$ the external forces, $\mathbf{B}$ a signed Boolean matrix mapping the matching DoFs, where $\mathbf{B}^{\mathrm{T}}\boldsymbol{\lambda}$ represents the interface forces, $\boldsymbol{\lambda}$ being the interface force intensities. The block matrix $\mathbf{Y}^{\mathrm{A|B}}$ holds the admittances of both substructure A and B. The admittance functions are always functions of ω, but here that is left out for compactness. By inserting the first equation into the second, solving for $\boldsymbol{\lambda}$, and reinserting the $\boldsymbol{\lambda}$ back into the first equation, the coupled response $\tilde{\mathbf{Y}}^{\mathrm{AB}}$ can be be obtained:

$$\tilde{\mathbf{Y}}^{\mathrm{AB}} = \left[\mathbf{I} - \mathbf{Y}^{\mathrm{A|B}}\mathbf{B}^{\mathrm{T}}\left(\mathbf{B}\mathbf{Y}^{\mathrm{A|B}}\mathbf{B}^{\mathrm{T}}\right)^{-1}\mathbf{B}\right]\mathbf{Y}^{\mathrm{A|B}}. \tag{2}$$

Note, it is a *dual* approach, since the original DoFs are retained, meaning that $\tilde{\mathbf{Y}}^{\mathrm{AB}}$ contains redundant information. The connected DoFs have per definition identical deformation. The redundancy can be removed by taking only the unique DoFs of $\tilde{\mathbf{Y}}^{\mathrm{AB}}$.

In the case of actual structures, a virtual point (VP) is often applied to connect two structures [3], since we often can't measure the full response at the actual interface. The idea is to ignore complex contact surfaces and not try to match every degree of freedom between the two structures, but instead relax the problem to a single virtual point (VP). We let VP have six DoFs: $\mathbf{q} = [q_X,\, q_Y,\, q_Z,\, q_{\theta_X},\, q_{\theta_Y},\, q_{\theta_Z}]^{\mathrm{T}}$, these DoFs are now the interface, and represent the interface deformation modes. Three translations and three rotations. Ultimately, we seek two transformation matrices to transform our actual measurement to collocated measurements at the VP:

$$\mathbf{Y}_{\mathbf{qp}} = \mathbf{T}_u\mathbf{Y}_{\mathrm{mea}}\mathbf{T}_f^{\mathrm{T}}, \tag{3}$$

where the subscript $\mathbf{p}$ represent the six virtual forces and moments, and $\mathbf{Y}_{\mathrm{mea}}$ are the measured frequency response functions of the non-matching interface DoFs. It is most likely not a quadratic matrix, and not symmetric, unless in the rare case that all impacts are driving point impacts. The goal of the transformation is to gain a symmetric 6×6 matrix $\mathbf{Y}_{\mathbf{qp}}$ with collocated DoFs. The idea is to place sensors near the

interface. If we assume only rigid motion between each sensor and the VP, measured displacements (or velocities/accelerations) can be transformed into the VP displacements by simple geometric conditions:

$$\begin{bmatrix} u_x^i \\ u_y^i \\ u_z^i \end{bmatrix} = \begin{bmatrix} e_{x,X} & e_{x,Y} & e_{x,Z} \\ e_{y,X} & e_{y,Y} & e_{y,Z} \\ e_{z,X} & e_{z,Y} & e_{z,Z} \end{bmatrix} \begin{bmatrix} 1 & 0 & 0 & 0 & r_Z & -r_Y \\ 0 & 1 & 0 & -r_Z & 0 & r_X \\ 0 & 0 & 1 & r_Y & -r_X & 0 \end{bmatrix} \mathbf{q} \quad \Rightarrow \quad \mathbf{u}^i = \mathbf{R}_u^i \, \mathbf{q}, \tag{4}$$

where $\boldsymbol{u}^i$ are measured displacements of sensor i near the interface, and $\boldsymbol{q}$ relates to $\boldsymbol{u}^i$ via the reduction matrix $\mathbf{R}_u^i$. The orientation of a sensor in x, in the global coordinate system, is $[e_{x,X},\, e_{x,Y},\, e_{x,Z}]^{\mathrm{T}}$ (and so forth for the other directions), and r_X, r_Y, r_Z are the arm lengths between sensor i and the VP, as demonstrated in Figure 1.

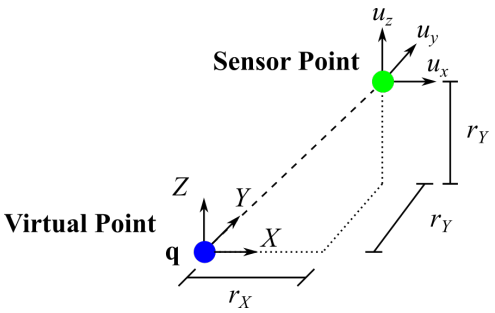

Figure 1: Concept of virtual point transformation of sensor data. Here the orientation matrix $\mathbf{e}$ is just a matrix of ones, since the sensor orientation aligns with the virtual point.

To predict the rotations in all three directions at least three triaxial sensors are needed $i > 2$. The problem then becomes an overdetermined system (a least square problem):

$$\begin{bmatrix} \mathbf{u}^1 \\ \mathbf{u}^2 \\ \mathbf{u}^3 \\ \vdots \end{bmatrix} = \begin{bmatrix} \mathbf{R}_u^1 & & & \\ & \mathbf{R}_u^2 & & \\ & & \mathbf{R}_u^3 & \\ & & & \ddots \end{bmatrix} \boldsymbol{q} + \boldsymbol{\mu} \quad \Rightarrow \quad \mathbf{u} = \mathbf{R}_u \, \mathbf{q} + \boldsymbol{\mu} \tag{5}$$

where $\boldsymbol{\mu}$ is the error. In the case of SLDV data, we now have the option of having a high number of measurements $i >> 3$ for the VP. However, after the reduction, the connection will remain a 6-Dof connection. We wish to arrive at a $\mathbf{T_u}$, as stated in equation (3). A solution minimizing the error $\boldsymbol{\mu}$ in the least square sense is [4]:

$$\mathbf{q} = \left(\mathbf{R}_u^{\mathrm{T}} \mathbf{R}_u\right)^{-1} \mathbf{R}_u^{\mathrm{T}} \mathbf{u}, , \qquad \mathbf{T}_u = \left(\mathbf{R}_u^{\mathrm{T}} \mathbf{R}_u\right)^{-1} \mathbf{R}_u^{\mathrm{T}}, \tag{6}$$

It is possible, and useful to add a symmetric weighting function $\mathbf{W}$ into the equation, making it possible to weigh some measurements higher than other when minimising [4].

Now on to the forces. We now seek $\mathbf{T}_f^{\mathrm{T}}$. Estimating the forces may appear like estimating the displacements, but it is fundamentally different. The displacements are unique. It is easiest to explain with a single parameter: Given a single displacement u_x^1, there is only one solution to q_X and $q_{X,\theta}$. That is not the case for forces. Infinite forces $\mathbf{f}$ can impose the same force and moment in the generalized coordinates $\mathbf{p}$. We look to find a force transformation matrix $\mathbf{T}_f^{\mathrm{T}}$ that transforms a given load in the generalized forces $\mathbf{p}$, to an equivalent vector of input forces $\mathbf{f}$ [3]:

$$\mathbf{f} = \mathbf{T_f}^{\mathrm{T}} \mathbf{p}, \tag{7}$$

with the requirement that

$$\mathbf{R}_f^i \mathbf{f} \stackrel{!}{=} \mathbf{p}, \tag{8}$$

We can therefore write:

$$\begin{bmatrix} p_x \\ p_y \\ p_z \\ p_{\theta_x} \\ p_{\theta_y} \\ p_{\theta_z} \end{bmatrix} = \begin{bmatrix} 1 & 0 & 0 & \\ 0 & 1 & 0 & \\ 0 & 0 & 1 & \\ & 0 & r_Z^f & -r_Y^f \\ & -r_Z^f & 0 & r_X^f \\ & r_Y^f & -r_X^f & 0 \end{bmatrix} \begin{bmatrix} e_{x,\,X} \\ e_{y,\,Y} \\ e_{z,\,Z} \end{bmatrix} f^i \quad \Rightarrow \quad \mathbf{p} = \mathbf{R}_f^{\mathrm{T},i}\, \mathbf{f}^i, \tag{9}$$

where $[e_X,\, e_Y,\, e_Z]^{\mathrm{T}}$ describes the direction of the impact in the VP coordinate system X, Y, Z. The f^i is the force intensity, and $\mathbf{p}$ is the virtual force vector, consisting of three forces and three moments. We have that $r_X^f,\, r_Y^f,\, r_Z^f$ are the arm lengths from the impact to the virtual point. In the special case of driving point excitation, the impact is in the same position as the sensor, and the distances to the virtual point would be the same. In that case, $\mathbf{R}_f^{\mathrm{T},i}$ is the transpose of $\mathbf{R}_u^i$. It is difficult in practice to make only driving point measurements, but for that reason it is standard to write the matrix with an transpose notation [3]. We can now add more forces and build a matrix system:

$$\mathbf{p} = \begin{bmatrix} \mathbf{R}_f^1 & & & \\ & \mathbf{R}_f^2 & & \\ & & \mathbf{R}_f^3 & \\ & & & \ddots \end{bmatrix} \begin{bmatrix} \boldsymbol{f}^1 \\ \boldsymbol{f}^2 \\ \boldsymbol{f}^3 \\ \vdots \end{bmatrix} \quad \Rightarrow \quad \mathbf{p} = \mathbf{R}_f^{\mathrm{T}}\, \boldsymbol{f} \tag{10}$$

Unlike, displacement transformation, we have under determined system. Infinitely many $\boldsymbol{f}$ can give a solution. We now now seek an optimal solution, in minimizing $\mathbf{f}^{\mathrm{T}}\mathbf{f}$, while subjected to $\mathbf{R}_f^{\mathrm{T}}\mathbf{f} - \mathbf{p} = \mathbf{0}$:

$$\mathbf{f} = \mathbf{T}_f^{\mathrm{T}}\mathbf{p}, \qquad \mathbf{T}_f^{\mathrm{T}} = \mathbf{R}_f \left(\mathbf{R}_f^{\mathrm{T}}\mathbf{R}_f\right)^{-1},$$

Again, it is possible to refine the transformation matrix by adding a weight matrix, weighting some impacts higher than others [4]. With the transformation matrices defined, we can directly apply equation (3) to get the collocated FRFs at the VP. A way to test the quality of the transformations is to look at the reciprocity. With the transformation, the 6×6 system has perfectly collocated degrees of freedom, so the off-diagonal terms should be mirrors of each other. To perform the above-explained VP operation, we use the open-source python-based software PyFBS [5].

2. NUMERICAL FRAMEWORK

Before an SLDV experiment is possible, a numerical framework suited for SLDV data must be devised. With the known AB benchmark [5], shown in Figure 3, we can exemplify common challenges with FBS and VP assumptions. It is important to place input forces and sensors at optimal positions, exciting all the rigid body modes of the interface. Measurements on substructure A are easy to plan, as there are no local, flexible modes at the interface. It is a rigid bar. However, substructure B has two cantilever-plate-like parts with bending modes within our range of interest (0-2000 Hz). When A and B are rigidly connected (cf. [6] for a case of coupling with flexible springs at the VP), these modes no longer exist. When planning the measurements of B, we want to limit the excitation of these local flexible modes.

Figure 2 shows an example of how a classical accelerometer setup could look and how an SLDV setup could look. The accelerometer setup has four mounted sensors and 13 impact points on each interface. With an SLDV, we can only measure perpendicular to the plane [7]. The new SLDV has 30 laser points perpendicular to each of the three surface directions, giving 90 outputs for the VP, with six forcing positions. An SLDV scans a surface really fast; 10 points take no more than 30 seconds to measure (varies depending on frequency resolution and how many averages are made). Therefore, increasing the grid from 30 to 50 points would be no problem, as the main experimental burden is in setting up the experiment rather than the actual measurement time. However, with a VP reduction, there is a limit to

the effect of more measurement points; what is more important is the position of the measurement points.

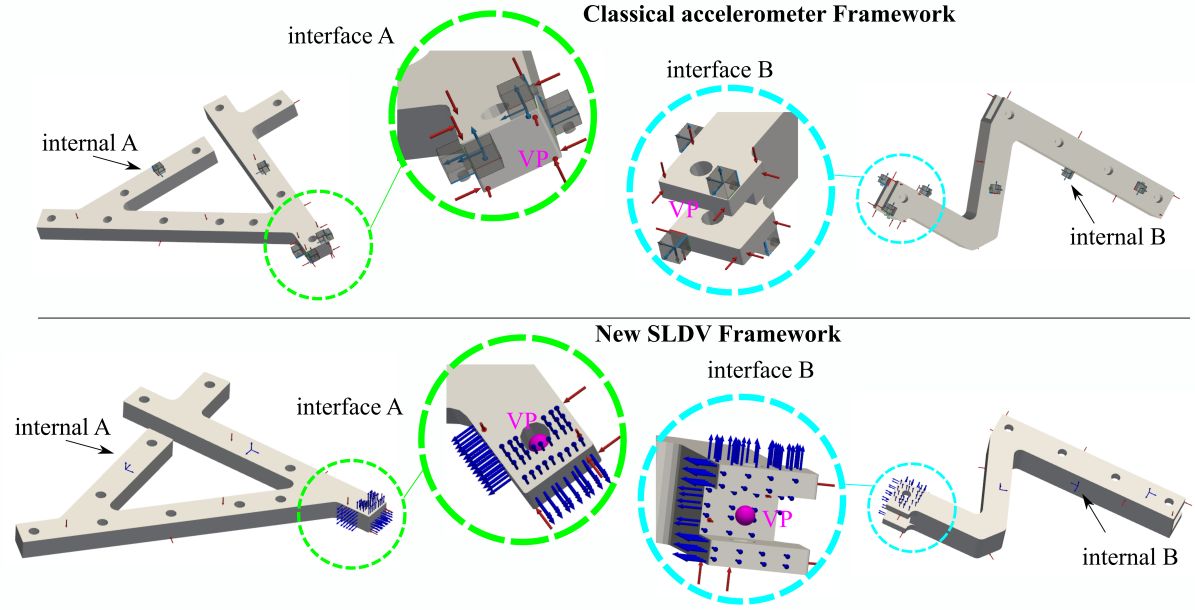

Figure 2: Measurements at the interface are transformed to the VP. The goal is to find out if SLDV can do better than accelerometers. Blue arrows: accelerometer/laser measurements: Red arrows: impacts/PZ. The transformation is based on the interface measurements. The internal measurements are left in their orginal positions, but part of the coupling.

Figure 3 shows an excerpt of the results from the numerical SLDV coupling. The FRF illustrated is an internal degree of freedom, as marked on the structure. It is evident that the SLDV-coupled FRF fits better with the reference (the reference is made by generating the FRF from a solid AB structure) than the accelerometer-based coupling. A reason is that it is possible to measure with the laser in points that are hard to reach with an accelerometer. The assumption is that the forcing can be done even in small spaces where a hammer impact cannot be placed. Overall, the numerical SLDV-coupled responses obtain good coherence to the reference (>0.8). However, it is not impressively better than the coherence obtainable with fewer 3D accelerometers and more impacts.

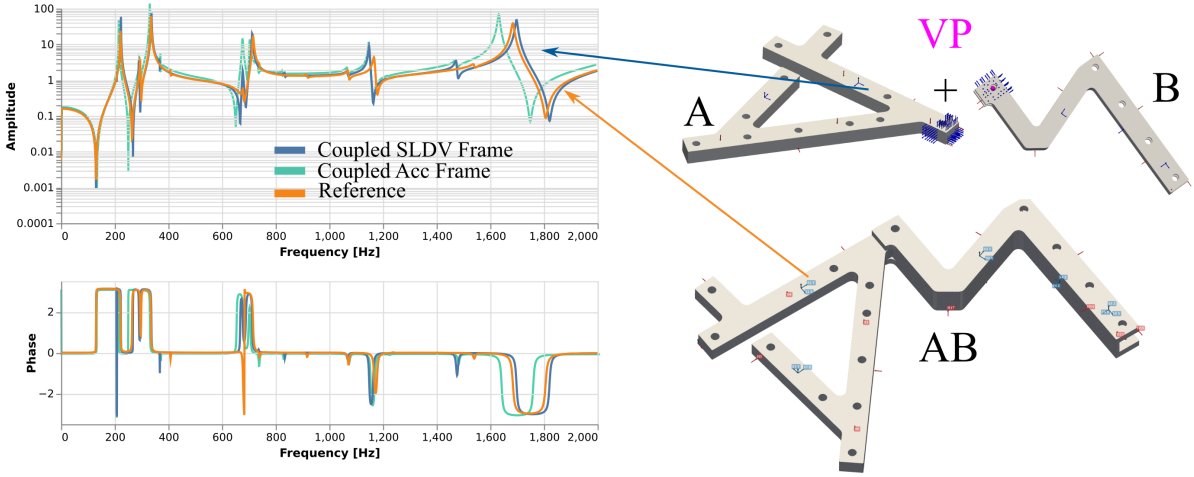

Figure 3: Left: Example FRF of coupled response (measured on A, after impact on A). Upper right: Coupled benchmark structure. Lower right: Interface measurements on A and B used for the VPT. Blue arrows represent SLDV points. Red excitation points.

3. CHALLENGES IN CARRYING OUT AN EXPERIMENT

There are some fundamental challenges when using an SLDV for FBS:

- Attaching a shaker/piezoelectric actuator can be cumbersome - and six positions are needed for each substructure to make VP transformation possible
- A force transducer is ideally required, as FBS only works with FRFs, not with auto spectrums
- The SLDV can only measure in one direction at a time (unlike a 3D accelerometer), meaning that the setup or SLDV must be rotated, and the measurement repeated to record all channels for all excitations.

This list reveals the cumbersomeness. However, there are options on how to overcome them. The shaker attachment can be made easier by placing the shaker in a stand that can easily be moved around. If we have a 3D structure, we must measure the velocities on three surfaces for six different impacts. As we can only measure one surface at a time, it means $6 \times 3 = 18$ measurement per structure. In comparison, the hammer-accelerometer measurements require approximately 12×3 hammer hits (12 positions, three repetitions). As a hammer hit is easier, the SLDV setup is still more cumbersome. A way to lessen the experimental burden could be to use hybrid modelling. E.g. the SEMM method [8], combining a numerical model with experiments. The concept is to use the numerically generated data, as the data generated in the previous section, but then 'replace' some of the information with experimental data. The SEMM procedure enforces equilibrium, so replacing some numerical FRFs with experimental FRFs will affect the whole numerical model, giving a new hybrid model. Another testing possibility could be to scan the interface from an angle, thus allowing a scan of all three surfaces in one go. The problem with this approach is that it may be difficult to estimate the exact angle of the laser w.r.t. the test object, and the angle is needed to get the right orientation matrix $\mathbf{e}$.

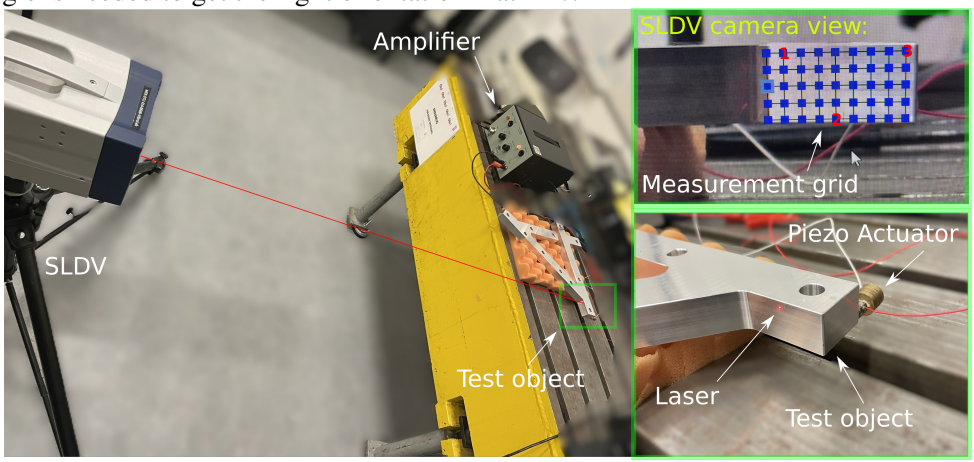

Figure 4: Left: full view of experimental setup. The amplifier drives the piezo electric actuator (PZ). Lower right: Zoom on test object. PZ is super glued on the back of the structure. Upper right: The defined measurement grid: the laser sweeps over the blue points on the surface.

4. EXPERIMENTAL SETUP AND RESULTS

A preliminary experiment is conducted to identify if it is even possible to get reliable data from an SLDV to use for FBS coupling. Figure 4 shows the setup. Substructure A is placed on foam, to mimic free-free boundary conditions. The surface to be tested is placed overhanging the foam, to ensure the foam is not obstructing the view of the laser. A piezo electric actuator (PZ) NAC2012-H6 (from Noliac) is glued to the back lower outer corner of the substructure. The PZ has only a 5×5 mm surface. The smaller the contact surface of the PZ, the closer the excitation is to a numerical point excitation. The PZ is a small stack piezo (height 6mm), where small ring masses are glued onto. These masses are added for counter mass. The bigger the mass the larger the force. However, adding mass also lowers the natural frequency of the actuator itself, and that still needs to be significantly above the measurement range. The piezoelectric excitation signal is generated within the PSV Polytec SLDV software. A pseudo random

signal from 0-2000 kHz. The generated signal is amplified with an B&K 2706 amplifier. This means the precise input force is unfortunately unknown. An option can be the add a force transducer between the piezo and the structure, but the force transducers we have at hand have very larger surfaces, making it inconvenient. The SLDV software automatically scans over the defined grid points (Figure 4 upper right). Each data point is an average over three measurements (the H1 estimator). The test is made with 6400 frequency lines, giving a resolution of 0.3125 Hz. The test of the 5x9 grid took about 2 minutes for the SLDV to carry out.

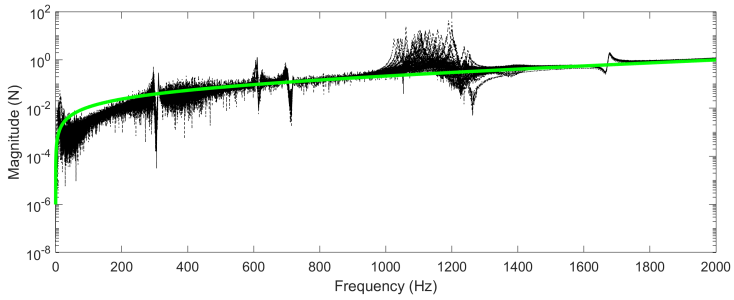

Figure 5: Black lines: Ratio between experimental magnitude and numerical magnitude for all 45 measurement points. Green line: exponential fit used for scaling the experimental data. The drop at lower frequencies can be explained by the PZ's lacking efficiency in that range.

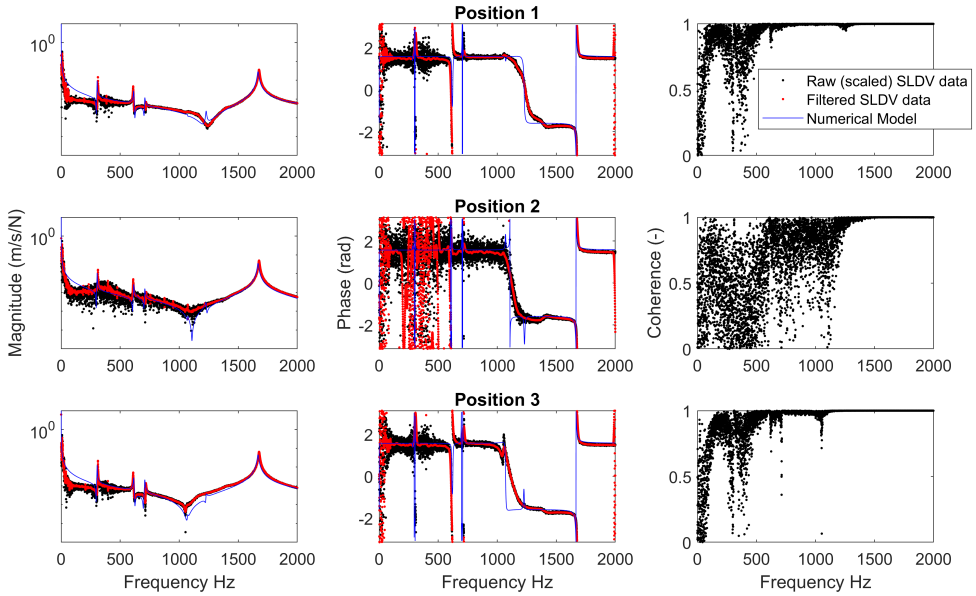

Figure 6: Measured response magnitude and phase, and coherence (the experimental data is a mean over three repetitions) for three different measurement positions, c.f. Figure 4 for position 1, 2 and 3 on the interface. The numerical model (blue lines) predictions are included for comparison. The red dots is the data after filtering.

As the force is not measured (the experimental FRF's are scaled with the ideal generated output), we apply a workaround. Using the numerical model, we have the expected FRFs (assuming a modal damping of 0.003); dividing the measured SLDV responses with the equivalent numerical responses indicates the actual forcing. Figure 5 shows the ratio between all 45 responses. The spikes express the slight deviation between model and experiment resonances and should be disregarded here, but the overall trend indicates the actual force put into the structure. PZs work poorly at low frequencies; a rule of thumb is that the input energy decreases significantly below 1000 Hz, which we also see here. We estimate the input force by fitting an exponential function (the green curve). As all 45 responses very much follow the same behaviour, it appears to be a reasonable assumption. An exponential function does not fully represent the forcing level below 200 Hz, but based on a single continuous function, it is good fit, ensuring that the force scaling does not drop below zero. Figure 6 shows a selection of the 45

recorded FRFs (after scaling), compared to the numerical model. The experimental FRFs are noisier at lower frequencies than what we normally see when using accelerometer and hammer testing. However, decent responses are obtained by post-processing filtering (red curves). The filtering, in this case, is based on Gaussian smoothing. The magnitude og phase are filtered separately. We smooth the magnitude data over 100 frequency lines, but skip the resonance peaks. The phase is smoothed w.r.t. to the measured coherence. If the coherence at a frequency is low, that phase value is weighted lower when smoothing over 100 frequency lines. Other filtering options may be more efficient, but the red lines show, that much can be achieved by filtering the experimental data, and in future works it is recommended to apply some sort of filtering. In conclusion, the experimental data was surprisingly fast to obtain and analyse, giving confidence that an entire measurement campaign is achievable.

5. CONCLUSIONS

Designing an experimental FBS campaign with an SLDV has proven to be a more complex modification than expected. Several factors must be considered. For one, a single SLDV can only measure in one principal direction, unlike 3D accelerometers. Secondly, using a type of excitation other than a hammer excitation is necessary. E.g., a shaker or a piezo-electric patch. These are cumbersome to move around, so a good experiment requires that the excitation positions are well chosen. Furthermore, it is more difficult to obtain a reliable measurement of the force input (a PZ itself does not measure the force). Intuitively, more measurement points should give better coupling; however, this is only sometimes the case when using a VP assumption. The numerical model helps us identify what to measure experimentally. The initial anticipation was that using an SLDV would be much better than using accelerometers. From the numerical studies, the conclusions are, however, more nuanced. Benefits may be obtained, but SLDV measurements must be carefully designed. The VP connection is the primary limiting factor rather than the amount of measurement data at the interface. The next step is to consider using a more direct coupling approach instead of simplifying all the information down to a single virtual point. The preliminary experimental works show that it is possible to get FRF data of acceptable quality and that by using the numerical model data, the PZ's input force can be roughly estimated. Another future FBS SLDV application could be to use it for hybrid substructuring. As the SLDV can scan over an entire surface in very high resolution, comparing data with the numerical modal and using the extensive data to tune the numerical model could be interesting.

ACKNOWLEDGMENTS

This work is financially supported by a research grant (41392) from VILLUM FONDEN.

REFERENCES

[1] M S; Allen, D; Rixen, Maarten; van der Seijs, P; Tiso, T; Abrahamsson, and R. L. Mayes. *Substructuring in Engineering Dynamics*. Springer International Publishing, 2020. ISBN 303025531x, 3030255328.

[2] M Brøns and D J Rixen. Dynamic disturbance substructuring : localized nonlinear vibrations. In *Proceedings of ISMA2022 International Conference on Noise and Vibration Engineering and USD2022 International Conference on Uncertainty in Structural Dynamics*, 2022.

[3] M. Haeussler, S. W.B. Klaassen, and D. J. Rixen. Experimental twelve degree of freedom rubber isolator models for use in substructuring assemblies. *Journal of Sound and Vibration*, 474:9–11, 2020. ISSN 10958568. doi: 10.1016/j.jsv.2020.115253.

[4] M. Häußler and Daniel Jean Rixen. Optimal transformation of frequency response functions on

interface deformation modes. *Conference Proceedings of the Society for Experimental Mechanics Series*, pages 225–237, 2017. ISSN 21915652, 21915644. doi: 10.1007/978-3-319-54930-9_20.

[5] Tomaž Bregar, Ahmed El Mahmoudi, Miha Kodrič, Domen Ocepek, Francesco Trainotti, Miha Pogačar, Mert Göldeli, Gregor Čepon, Miha Boltežar, and Daniel J. Rixen. pyfbs: A python package for frequency based substructuring. *Journal of Open Source Software*, 7(69):3399, 2022. doi: 10.21105/joss.03399.

[6] Marie Brøns, Francesco Trainotti, and Daniel J. Rixen. A novel optimization framework using frequency-based substructuring for estimation of linear bolted joint stiffness and damping. *Mechanical Systems and Signal Processing*, 223(July 2024):111806, 2025. ISSN 10961216. doi: 10.1016/j.ymssp.2024.111806. URL https://doi.org/10.1016/j.ymssp.2024.111806.

[7] M. Brøns and J.J. Thomsen. Experimental testing of Timoshenko predictions of supercritical natural frequencies and mode shapes for free-free beams. *Journal of Sound and Vibration*, 459, 2019. doi: https://doi.org/10.1016/j.jsv.2019.114856.

[8] Steven W.B. Klaassen, Maarten V. van der Seijs, and Dennis de Klerk. System equivalent model mixing. *Mechanical Systems and Signal Processing*, 105:90–112, 2018. ISSN 10961216. doi: 10.1016/j.ymssp.2017.12.003. URL https://doi.org/10.1016/j.ymssp.2017.12.003.